PHYSICAL REVIEW B VOLUME 39, NUMBER 18 15 JUNE 1989-II

Experimental and theoretical studies of energy transfer in F-center–$OH^-(OD^-)$ defect pairs in KCl

G. Halama and K. T. Tsen
Department of Physics, Arizona State University, Tempe, Arizona 85287

S. H. Lin
Department of Chemistry, Arizona State University, Tempe, Arizona 85287

F. Lüty
Department of Physics, University of Utah, Salt Lake City, Utah 84112

J. B. Page
Department of Physics, Arizona State University, Tempe, Arizona 85287

(Received 10 November 1988; revised manuscript received 27 February 1989)

Anti-Stokes Raman spectroscopy has been employed to investigate energy-transfer processes in F-center–$OH^-(OD^-)$ -defect pairs in KCl. The experimental results demonstrate that at least a good part of the electronic excitation energy becomes transferred to the vibrational states of neighboring OH^- or OD^- ions. In contrast to the F-center–CN^--defect pairs in CsCl, only the lower ($n \leq 2$) vibrational energy levels of OH^- or OD^- are populated and detected. A model which considers the E-V transfer through dipole-dipole interactions is proposed to account for the observed experimental results.

I. INTRODUCTION

Recently, F-center–molecule defect complexes in ionic crystals such as alkali halides have attracted a considerable amount of attention.[1–7] This is partly because of their potential application as solid-state systems capable of tunable near-infrared laser operation and partly because of the interesting physics they bring about. It is well known that an F center in ionic crystals can be associated with a variety of anionic, cationic, or vacancy point defects. For example, optical aggregation of an F center in highly OH^--doped KCl crystals at $T \sim 240$ K leads to the formation of F-center–OH^--ion pairs.[2] In contrast to F-center–CN^-- or F-center–OH^- defect pairs in cesium halides,[3,7] in which the electronic absorption is split into two bands, these pair defects in host crystals of NaCl structure are characterized by a single broadened and red-shifted electronic absorption. In addition, measurements of the $F_H(OH^-)$ center ground-state-bleach recovery kinetics under pulsed laser excitation in KCl show that the nonradiative deexcitation of the F_H electron occurs extremely rapidly, i.e., on the order of subnanoseconds.[8] Under excitation of the electronic transitions of $F_H(CN^-)$ defects by a visible light, one observed an energy transfer into CN^- vibrational energy as evidenced either by the 4.8-μm CN^- vibrational emission[1,3] or by the detection of the population of various excited CN^- vibrational states in anti-Stokes Raman-scattering experiments.[6] In contrast to the case of F-center–CN^- defect pairs, no trace of the OH^- stretching vibration emission has been observed in a variety of host crystals, particularly, in KCl.[2,7] Therefore, the most basic remaining unanswered questions are: Is there electronic-vibrational (E-V) transfer into the OH^- defect? If the answer turns out to be positive, then what is the coupling or energy-transfer process through which the F_H electron loses its excitation energy so efficiently to the OH^--ion neighbor?

Anti-Stokes Raman scattering has been demonstrated to be a viable technique for probing energy-transfer processes in F-center–CN^- defect pairs in CsCl.[6] In this paper, we have used this spectroscopy to examine the energy-transfer mechanism in F-center–OH^- (or OD^-) defect pairs in KCl. We demonstrate for the first time that at least a good part of the F-center electronic excitation energy is transferred into the vibrational states of the attached OH^- or OD^-. A model which considers the E-V transfer through dipole-dipole interactions (i.e., the Dexter-Förster mechanism) is proposed to account for the observed experimental results.

II. EXPERIMENTAL TECHNIQUE AND SAMPLES

The same beam from the second harmonic of a cw mode-locked yttrium-aluminum-garnet (YAG) laser operating at repetition rate of 76 MHz is used to excite the F-center electron and for *in situ* probing of the vibrational population of the OH^- or OD^- through anti-Stokes Raman scattering. The average power of the laser is about 1 W and the pulse width is ~ 60 ps. The laser beam is focused onto the surface of the sample with a spot size of ~ 100 μm. In order to collect as much scattered light as possible, 90° scattering geometry is employed. The anti-Stokes Raman signal is analyzed by a double monochromator and a standard photon-counting system. The sample is kept in contact with a constant flow of cold He gas (~ 10 K). The temperature of the laser-irradiated area is estimated to be ≈ 60 K, which is larger than 10 K because of the very high average laser power (~ 1 W) used in the experiments.

The $F_H(\mathrm{OH}^-)$ and $F_H(\mathrm{OD}^-)$ crystals studied in this work were grown by the Czochralski technique and additively colored at the University of Utah. They contain about 2×10^{17} cm^{-3} F centers and about 5×10^{19} cm^{-3} OH$^-$ or OD$^-$. The sample used was first quenched at a temperature of $\sim$250 °C and carefully transferred in the dark at room temperature into the cryostat. At $T\simeq-30$ °C the F centers were aggregated into $F_H(\mathrm{OH}^-)$ or $F_H(\mathrm{OD}^-)$ pairs by exposure of the crystal to a flash lamp for about 20 min.

III. EXPERIMENTAL RESULTS

We present in this work measurements on two types of defect systems, i.e., $F_H(\mathrm{OH}^-)$ and $F_H(\mathrm{OD}^-)$.[9] Figure 1 shows the experimental results obtained for $F_H(\mathrm{OH}^-)$ defects in KCl at $T\simeq60$ K. Three anti-Stokes Raman lines denoted by A, B, and C appear at 3650, 3600, and 3410 cm^{-1}. These Raman lines are extremely weak but remain observable up to $T\simeq160$ K. The highest energy line A lies very close to the stretching mode frequency $\nu_1=3643$ cm^{-1} of the isolated OH$^-$ defect. We attribute the two lower energy lines B and C to the $v=1\rightarrow0$ and $v=2\rightarrow1$ vibrational OH$^-$ transitions in the $F_H(\mathrm{OH}^-)$ complex. Apparently, the presence of a "soft" F-center neighbor lowers slightly the OH$^-$ stretching frequency relative to that of the isolated defect,[7] while our observed anharmonic shift $\nu(B)-\nu(C)\simeq190$ cm^{-1} coincides closely with the one ($\simeq170$ cm^{-1}) observed for isolated OH$^-$ defects.[10]

Because (1) the crystal contains a very high concentration of OH$^-$ and (2) the relative intensity of Raman lines A and B does not change significantly when the temperature varies from 60 to 160 K, we believe that the presence of the additional line A indicates that, besides the close F/OH$^-$ pair, a more widely separated F/OH$^-$ pair configuration exists, characterized by an OH$^-$ frequency nearly equal to that of the isolated OH$^-$ ion and by a slightly weaker E-V transfer process so that only the $v=1$ state has been populated.

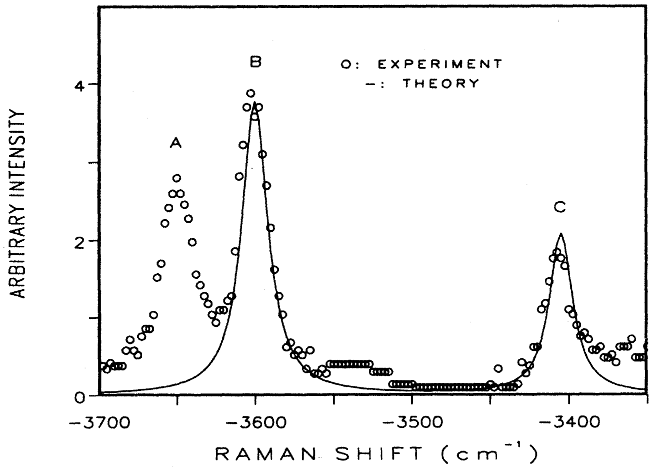

FIG. 1. Comparison of experimental and theoretical resonance Raman spectra of $F_H(\mathrm{OH}^-)$ defect pairs for highly doped OH$^-$ in KCl.

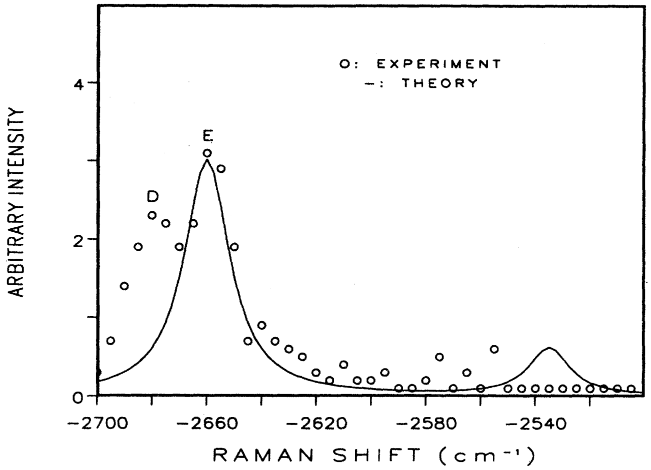

FIG. 2. Comparison of experimental and theoretical resonance Raman spectra of $F_H(\mathrm{OH}^-)$ defect pairs for highly doped OD$^-$ in KCl.

Figure 2 shows the anti-Stokes Raman spectrum for $F_H(\mathrm{OD}^-)$ defects in KCl at $T\simeq60$K. Two extremely weak Raman lines labeled D and E at 2680 and 2660 cm^{-1} are detected. Again, we think that there exist two types of F/OD$^-$ configuration. Line D is located very close to the frequency of the isolated OD$^-$ defect and is the result of energy transfer between the excited F center and a distant OD$^-$ defect, whereas line E originates from a near $F_H(\mathrm{OD}^-)$ pair defect.

We have also carried out polarization measurements on these crystals. Under ⟨100⟩ polarized excitation light, all three bands of $F_H(\mathrm{OH}^-)$ and the two bands of $F_H(\mathrm{OD}^-)$ centers show about the same Raman intensity for perpendicular ⟨010⟩ as for parallel ⟨100⟩ polarizations. These results are quite different from those obtained for $F_H(\mathrm{CN}^-)$ defect pairs in which a Raman signal associated with parallel polarization has been found to be much stronger than a perpendicular one.[6] Experiments are under way to clarify this observation.

IV. THEORY

The observed differential scattering cross section per unit solid angle per unit frequency is given by

$$\frac{d^2\sigma}{d\Omega\, d\omega_s}=\sum_i \rho_i \frac{d^2\sigma_i}{d\Omega\, d\omega_s}\,, \qquad (1)$$

where $d^2\sigma_i/d\Omega\, d\omega_s$ is the differential scattering cross section for the ith state, ρ_i is the initial population of ith state, the summation over i covers the initial states, ω_s is the scattered light frequency, and Ω is the solid angle.

The above expression for the resonance-Raman scattering (RRS) cross section is quite general; for the time-resolved RRS,[11] ρ_i is a function of time describing the time evolution of the system. In the present work, ρ_i represents the steady-state population of the vibrational states of OH$^-$ or OD$^-$ in the F-center–OH$^-$(OD$^-$) systems due to the EV transfer, and vibrational emission and relaxation. In the following, we show how to determine

ρ_i by using the density-matrix method (i.e., the master equation approach) and how to calculate the single-level RRS cross section.

A. Time evolution of the density matrix

First let us determine the population of the various states by using the stochastic Liouville equation[12]

$$\frac{d\rho}{dt} = -iL\rho - \frac{i}{\hbar}[V,\rho] - \Gamma\rho \ , \tag{2a}$$

where ρ is the density-matrix operator, L is the Liouville operator of the system, V is the interaction potential of incident radiation field given by $D(\omega_r)\exp(-i\omega_r t) + D(-\omega_r)\exp(i\omega_r t)$ with ω_r being the frequency of the incident radiation, and Γ is the damping operator which describes the relaxation and dephasing of the system.

We would like to apply the Liouville equation to the energy-level scheme shown in Fig. 3. In our model we assume that the system is at the very lowest temperatures, the incident radiation pumps the system from the electronic ground state (g) to the electronic excited state (E) of the F center from where it very rapidly relaxes into the relaxed excited state (a) which has a long ($\approx 10^{-6}$ sec) radiative lifetime. Due to the perturbing Hamiltonian H', it can decay from this a state to various vibrational states, $m, m-1, m-2, \ldots$, of OH$^-$ or OD$^-$. The wave functions of the system are given by the Born-Oppenheimer approximation. The time evolution of diagonal density-matrix element of the a state is given by

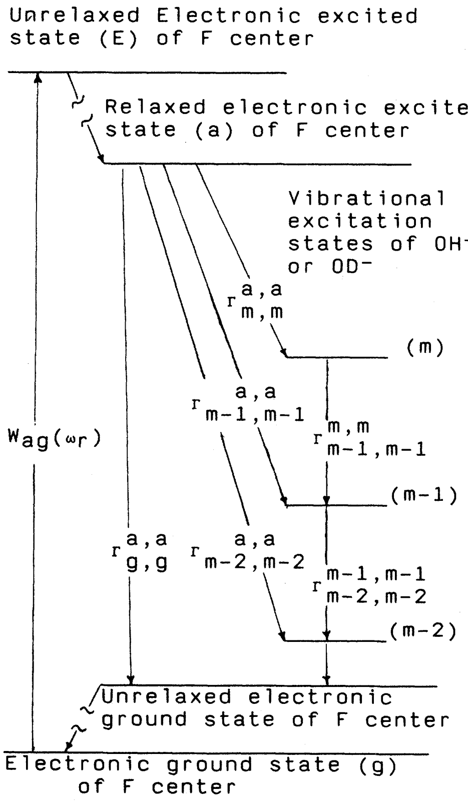

FIG. 3. Model of electronic-vibrational energy transfer in F_H(OH$^-$) and F_H(OD$^-$) defect pairs complexes in KCl.

$$\frac{d\rho_{aa}}{dt} + (i/\hbar)(V_{ag}\rho_{ga} - \rho_{ag}V_{ga}) + \Gamma^{aa}_{aa}\rho_{aa} = 0 \ , \tag{2b}$$

where $-\Gamma^{aa}_{aa} = \Gamma^{aa}_{gg} + \sum_m \Gamma^{aa}_{mm}$, ρ_{aa} is the diagonal density-matrix element for the a state, ρ_{ag} and ρ_{ga} are off-diagonal elements between the a state and g state, V_{ag} and V_{ga} describe the coupling of the radiation field to the system, and Γ^{aa}_{aa} is the decay constant for all the possible decays out of the excited state a. Now consider the off-diagonal elements between the a state and g state,

$$\frac{d\rho_{ag}}{dt} + i\omega_{ag}\rho_{ag} + (i/\hbar)V_{ag}(\rho_{gg} - \rho_{aa}) + \Gamma^{ag}_{ag}\rho_{ag} = 0 \ , \tag{2c}$$

where $\omega_{ag} = (E_a - E_g)/\hbar$, E_a and E_g are the eigenenergies of their respective states, and Γ^{ag}_{ag} equals the damping constant for these states. If we substitute for V and calculate the elements V_{ag} and V_{ga} and use the rotating wave and steady-state approximations, we get

$$\rho_{ag} = \frac{i(\rho_{gg} - \rho_{aa})}{\hbar} \left[\frac{D_{ag}(\omega_r)}{i(\omega_{ag} - \omega_r) + \Gamma^{ag}_{ag}} \right] , \tag{3}$$

where $D_{ag}(\omega_r) = \langle a | D(\omega_r) | g \rangle$. The substitute Eq. (3) into Eq. (2b) to get

$$\frac{d\rho_{aa}}{dt} + W_{ag}(\omega_r)(\rho_{aa} - \rho_{gg}) + \Gamma^{aa}_{aa}\rho_{aa} = 0 \ , \tag{4}$$

where $W_{ag}(\omega_r)$ represents the absorption rate constant

$$W_{ag}(\omega_r) = \frac{2/\hbar^2 |\langle a | D(\omega_r) | g \rangle|^2 \Gamma_{ag}}{\Gamma^2_{ag} + (\omega_{ag} - \omega_r)^2} \ , \tag{5}$$

where $\Gamma_{ag} = \Gamma^{ag}_{ag}$.

Then consider the matrix elements for the vibrational states

$$\frac{d\rho_{mm}}{dt} + \Gamma^{aa}_{mm}\rho_{aa} + \Gamma^{mm}_{mm}\rho_{mm} + \Gamma^{m+1,m+1}_{mm}\rho_{m+1,m+1} = 0 \ , \tag{6}$$

where the superscript or subscript m and a stands for the excitation level of the vibrational mode and the electronic excited state, respectively; Γ^{aa}_{mm} is the radiationless transition rate from the relaxed electronic excited state to the mth vibrational excitation, Γ^{mm}_{mm} is the transition rate for all possible decays out of the mth vibrational state, and $\Gamma^{m+1,m+1}_{m,m}$ is the transition rate from the $(m+1)$th vibrational excitation to the mth vibrational excitation.

Equations (4) and (6) will be the master equations used to analyze the experimental results either for time-resolved spectroscopy or steady-state spectroscopy. For the experimental results reported in this paper, we will use the steady-state solutions to Eqs. (4) and (6). Thus we obtain

$$\rho_{aa} = \frac{W_{ag}(\omega_r)\rho_{gg}}{W_{ag}(\omega_r) + \Gamma^{aa}_{aa}} \ , \tag{7}$$

$$\rho_{mm} = -\frac{\Gamma_{mm}^{aa}\rho_{aa} + \Gamma_{m,m}^{m+1,m+1}\rho_{m+1,m+1}}{\Gamma_{mm}^{mm}} . \tag{8}$$

From Eq. (8) we see that the mth vibrational level can be pumped from level a by the EV transfer and from the upper vibrational $m+1$ level by radiative or nonradiative vibrational relaxation processes. Next, we discuss the theoretical treatment of the EV transfer. Here we modify Förster's theory for electronic energy transfer,[13] i.e.,

$$D(\mathrm{el}^*) + A \rightarrow D + A(\mathrm{el}^*) . \tag{9}$$

The original treatment was for the case in which the electronically excited donor D transfers its electronic excitation to the acceptor A by the dipole-dipole interaction; after accepting the excitation energy the acceptor A becomes electronically excited. In our case, D is the F center and A is OH^- or OD^-. The F center is initially excited by optical absorption and the excited F center transfers part of its excitation energy to the OH^- (or OD^-), but the OH^- (or OD^-) is only vibrationally excited, i.e.,

$$D(\mathrm{el}^*) + A \rightarrow D + A(\mathrm{vib}^*) . \tag{10}$$

A similar situation is observed in the quenching of singlet O_2 by solvent molecules.[14,15(a)] Jang *et al.*[8] first qualitatively discussed the possibility of the application of this mechanism to the F-center–$\mathrm{OH}^-(\mathrm{OD}^-)$ problem. Fowler[15(b)] also applied this mechanism to the F-center–CN^- problem and found that it is not applicable to that system. In a forthcoming paper, we shall show that for the F-center–CN^- system, a different mechanism is required.

B. Energy transfer

In this section, we present the theoretical treatment of the EV transfer rate constant $-\Gamma_{mm}^{aa}$. We shall start with Fermi's Golden Rule expression for the electronic transition $a \rightarrow b$. The transition rate is given by

$$W_{a \rightarrow b} = \frac{2\pi}{\hbar} \sum_{v} \sum_{v'} P_{av} |\langle av|\hat{H}'|bv'\rangle|^2 \delta(E_{av} - E_{bv'}) , \tag{11}$$

where P_{av} is the Boltzmann factor and $\delta(E_{av} - E_{bv'})$ is the δ function. Using the adiabatic (i.e., Born-Oppenheimer) approximation,

$$|av\rangle = \Phi_a \Theta_{av} , \quad \Phi_a = \Phi_a^{(A)} \Phi_a^{(D)} , \quad \Theta_{av} = \Theta_{av}^{(A)} \Theta_{av}^{(D)} , \tag{12}$$

$$|bv'\rangle = \Phi_b \Theta_{bv'} , \quad \Phi_b = \Phi_b^{(A)} \Phi_b^{(D)} , \quad \Theta_{bv'} = \Theta_{bv'}^{(A)} \Theta_{bv'}^{(D)} , \tag{13}$$

where (Φ_a, Φ_b) represent the electronic wave functions while $(\Theta_{av}, \Theta_{bv'})$ denote the vibrational wave functions, we obtain

$$W_{a \rightarrow b} = \frac{2\pi}{\hbar} \sum_{v} \sum_{v'} P_{av} |\langle \Theta_{av}|H'_{ab}|\Theta_{bv'}\rangle|^2 \delta(E_{av} - E_{bv'}) , \tag{14}$$

where

$$H'_{ab} = \frac{1}{\epsilon R^3} \left[(\boldsymbol{\mu}_A \cdot \boldsymbol{\mu}_D) - \frac{3(\mathbf{R} \cdot \boldsymbol{\mu}_A)(\mathbf{R} \cdot \boldsymbol{\mu}_D)}{R^2} \right] , \tag{15}$$

R is the distance between the donor and acceptor (i.e., between the F center and OH^- or OD^-),

$$\boldsymbol{\mu}_D = \langle \Phi_a^{(D)} | \boldsymbol{\mu} | \Phi_b^{(D)} \rangle \quad (b \neq a) , \tag{16}$$

$\boldsymbol{\mu}$ is the dipole operator, $\boldsymbol{\mu}_D$ is the transition moment from relaxed electronic excited state to the electronic ground state of the donor (i.e., F-center), and

$$\boldsymbol{\mu}_A = \langle \Phi_a^{(A)} | \boldsymbol{\mu} | \Phi_b^{(A)} \rangle = \langle \Phi_a^{(A)} | \boldsymbol{\mu} | \Phi_a^{(A)} \rangle , \tag{17}$$

where $\boldsymbol{\mu}_A$ is the dipole moment of the acceptor (i.e., OH^- or OD^-) because the electronic wave function of OH^- or OD^- remains unchanged during the transition or

$$\boldsymbol{\mu}_A = \boldsymbol{\mu}_A^0 + \left[\frac{d\boldsymbol{\mu}_A}{dx} \right]_0 x + \cdots , \tag{18}$$

where x denotes the vibrational displacement of the diatomic acceptor. In Eq. (15), ϵ represents the dielectric constant.

For our purpose, we shall express the EV transfer rate constant in terms of an energy gap, transition moments, Huang-Rhys constant, etc.

H'_{ab} can be written as

$$H'_{ab} = \frac{1}{\epsilon R^3} |\boldsymbol{\mu}_D| \left| \left[\frac{d\boldsymbol{\mu}_A}{dx_0} \right] \right| \eta_{AD} x , \tag{19}$$

where η_{AD} denotes the relative orientation factor for A and D. For our problem we are concerned with the transition $an \rightarrow bn'$, i.e.,

$$W_{an \rightarrow bn'} = \frac{2\pi}{\hbar} \frac{|\boldsymbol{\mu}_D|^2 n_{AD}^2}{\epsilon^2 R^6} \left| \left[\frac{d\boldsymbol{\mu}_A}{dx} \right]_0 \right|^2 x_{nn'}^2 \times \sum_{v} \sum_{v'} P_{av}^{(D)} |\langle \Theta_{av}^{(D)} | \Theta_{bv'}^{(D)} \rangle|^2 \times \delta(E_{av}^{(D)} - E_{bv'}^{(D)} + n\hbar\omega - n'\hbar\omega) , \tag{20}$$

where $E_{av}^{(D)} = E_a^{(D)} + \sum_j (v_j + \frac{1}{2})\hbar\omega_j$ and $E_{bv}^{D} = E_b^{(D)} + \sum_j (v'_j + \frac{1}{2})\hbar\omega_j$ with $E_a^{(D)} = \hbar\omega_a^{(D)}$ and $E_b^{(D)} = \hbar\omega_b^{(D)}$ being the energy at the minima of electronic ground state and relaxed excited state, respectively; ω_j is the frequency of the jth mode of the Condon coupled oscillator to the donor (F center), and ω is the frequency of the stretching mode of the acceptor (i.e., OH^- or OD^-),

$$x_{nn'} = \langle n | x | n' \rangle \tag{21}$$

for OH^- or OD^-. Notice that Eq. (20) can be simplified as[16]

$$W_{an\to bn'}=\frac{1}{\hbar^2}\frac{|\mu_D|^2\eta_{AD}^2}{\epsilon^2R^6}\left|\frac{d\mu_A}{dx_0}\right|^2 x_{nn'}^2\frac{2\pi}{\left[\sum_j S_j\omega_j^2\coth\frac{\hbar\omega_j}{2kT}\right]^{1/2}}\exp\left[\frac{\left[\omega_a^{(D)}-\omega_b^{(D)}+n\omega-n'\omega-\sum_j S_j\omega_j\right]^2}{\left[2\sum_j S_j\omega_j^2\coth\frac{\hbar\omega_j}{2kT}\right]}\right], \tag{22}$$

where S_j denotes the dimensionless normal coordinate displacement for the jth mode, and that at $T=0$

$$W_{a0\to bn'}=\frac{1}{\hbar^2}\frac{|\mu_D|^2\eta_{AD}^2}{\epsilon^2R^6}\Bigg|\Bigg|\left[\frac{d\mu_A}{dx}\right]_0\Bigg|^2 x_{0n'}^2\left[\frac{2\pi}{\sum_j S_j\omega_j^2}\right]^{1/2}\exp\left[\frac{\left[\omega_a^{(D)}-\omega_b^{(D)}-n'\omega\sum_j\omega_jS_j\right]^2}{2\sum_j S_j\omega_j^2}\right]. \tag{23}$$

It follows that for the F-center/OH$^-$ or F-center/OD$^-$ system we have

$$\frac{W_{a0\to b2}}{W_{a0\to b1}}=\frac{|x_{02}|^2}{|x_{01}|^2}\exp\left\{\left[2\sum_j S_j\omega_j^2\right]^{-1}\left[\left[\omega_a^{(D)}-\omega_b^{(D)}-\omega-\sum_j S_j\omega_j\right]^2-\left[\omega_a^{(D)}-\omega_b^{(D)}-2\omega-\sum_j S_j\omega_j\right]^2\right]\right\}, \tag{24}$$

and that for the comparison between the F-center/OH$^-$ and F-center/OD$^-$ systems we find

$$\frac{W_{a0\to b1}(\mathrm{OD})}{W_{a0\to b1}(\mathrm{OH})}=\frac{|x_{01}(\mathrm{OD})|^2}{|x_{01}(\mathrm{OH})|^2}\exp\left\{-\left[2\sum_j S_j\omega_j^2\right]^{-1}\left[\left[\omega_a^{(D)}-\omega_b^{(D)}-\omega_{\mathrm{OD}}-\sum_j S_j\omega_j\right]^2-\left[\omega_a^{(D)}-\omega_b^{(D)}-\omega_{\mathrm{OH}}-\sum_j S_j\omega_j\right]^2\right]\right\} \tag{25}$$

and

$$\frac{W_{a0\to b2}(\mathrm{OD})}{W_{a0\to b2}(\mathrm{OH})}=\frac{|x_{02}(\mathrm{OD})|^2}{|x_{02}(\mathrm{OH})|^2}\exp\left[-\frac{1}{\left[2\sum_j S_j\omega_j^2\right]}\left[\left[\omega_a^{(D)}-\omega_b^{(D)}-2\omega_{\mathrm{OD}}-\sum_j S_j\omega_j\right]^2-\left[\omega_a^{(D)}-\omega_b^{(D)}-2\omega_{\mathrm{OH}}-\sum_j S_j\omega_j\right]^2\right]\right]. \tag{26}$$

For harmonic oscillators we have

$$x_{n+1,n}^0=\left[\frac{\hbar(n+1)}{2\mu\omega}\right]^{1/2}=\left[\frac{(n+1)}{2\beta}\right]^{1/2}, \tag{27}$$

where $\beta=\mu\omega/\hbar=1/\hbar(\mu K)^{1/2}$, K being the force constant, μ the molecular reduced mass, and

$$\frac{|x_{n+1,n}^0(\mathrm{OD})|^2}{|x_{n+1,n}^0(\mathrm{OH})|^2}=\left[\frac{\mu_{\mathrm{OH}}}{\mu_{\mathrm{OD}}}\right]^{1/2} \tag{28}$$

or

$$\frac{W_{a0\to b1}(\mathrm{OD})}{W_{a0\to b1}(\mathrm{OH})}=\left[\frac{\mu_{\mathrm{OH}}}{\mu_{\mathrm{OD}}}\right]^{1/2}\exp\left\{-\left[2\sum_j S_j\omega_j^2\right]^{-1}\left[\left[\omega_a^{(D)}-\omega_b^{(D)}-\omega_{\mathrm{OD}}-\sum_j S_j\omega_j\right]^2-\left[\omega_a^{(D)}-\omega_b^{(D)}-\omega_{\mathrm{OH}}-\sum_j S_j\omega_j^2\right]\right]\right\}. \tag{29}$$

To calculate x_{02} we need to introduce anharmonicity, i.e.,

$$\psi_n=\psi_n^0+\sum_m{}'\frac{\langle\psi_m^0|\hat{H}'|\psi_n^0\rangle}{E_n^0-E_m^0}\psi_m^0+\cdots, \tag{30}$$

where ψ_n is the wave function of the perturbed oscillator, ψ_n^0, ψ_m^0 are wave functions of the unperturbed harmonic oscillator, and

$$\hat{H}'=a_3x^3+\cdots. \tag{31}$$

It follows that

$$x_{02}=\frac{x_{01}^{0}\langle\psi_1^0|\hat{H}'|\psi_2^0}{E_2^0-E_1^0}+\frac{x_{12}^{0}\langle\psi_1^0|\hat{H}'|\psi_0^0\rangle}{E_0^0-E_1^0}+\frac{x_{23}^{0}\langle\psi_3^0|\hat{H}'|\psi_0^0\rangle}{E_0^0-E_3^0}\ , \tag{32}$$

$$\langle\psi_1^0|H'|\psi_0^0\rangle=\frac{3\sqrt{2}}{4}\frac{a_3}{\beta^{3/2}}\ , \tag{33}$$

$$\langle\psi_3^0|H'|\psi_0^0\rangle=\frac{\sqrt{3}}{2}\frac{a_3}{\beta^{3/2}}\ , \tag{34}$$

$$\langle\psi_2^0|\hat{H}'|\psi_1^0\rangle=\frac{3a_3}{\beta^{3/2}}\ , \tag{35}$$

and

$$x_{02}^2=\frac{a_3^2\hbar^2}{2K^3\mu}\ . \tag{36}$$

Therefore we obtain

$$\frac{W_{a0\to b2}}{W_{a0\to b1}}=\frac{a_3^2\hbar}{\mu^3\omega^5}\exp\left\{\left[2\sum_j S_j\omega_j^2\right]^{-1}\left[\left[\omega_a^{(D)}-\omega_b^{(D)}-\omega-\sum_j S_j\omega_j\right]^2-\left[\omega_a^{(D)}-\omega_b^{(D)}-2\omega-\sum_j S_j\omega_j\right]^2\right]\right\} \tag{37}$$

and

$$\frac{W_{a0\to b2}(\mathrm{OD})}{W_{a0\to b2}(\mathrm{OH})}=\left[\frac{\mu_{\mathrm{OH}}}{\mu_{\mathrm{OD}}}\right]\exp\left\{-\left[2\sum_j S_j\omega_j^2\right]^{-1}\left[\left[\omega_a^{(D)}-\omega_b^{(D)}-2\omega_{\mathrm{OD}}-\sum_j S_j\omega_j\right]^2-\left(\omega_a^{(D)}-\omega_b^{(D)}-2\omega_{\mathrm{OH}}-\sum_j S_j\omega_j\right)^2\right]\right\}\ . \tag{38}$$

The anharmonicity constant a_3 can be estimated by using the Morse oscillator

$$V=V_d(1-e^{-ax})^2 \tag{39}$$

and

$$E_n=(n+\tfrac{1}{2})\hbar\omega-\chi_e(n+\tfrac{1}{2})^2\hbar\omega\ , \tag{40}$$

then

$$a_3=-V_d a^3,\quad K=2V_d a^2\ , \tag{41}$$

and

$$a_3^2=\frac{K^3}{8V_d}\ . \tag{42}$$

Here V_d is the dissociation energy. Notice that

$$\chi_e=\frac{\hbar\omega}{4V_d}\ , \tag{43}$$

$$a_3^2=\frac{K^3\chi_e}{2\hbar\omega}\ , \tag{44}$$

and

$$\frac{W_{a0\to b2}}{W_{a0\to b1}}=\tfrac{1}{2}\chi_e\exp\left\{\left[2\sum_j S_j\omega_j^2\right]^{-1}\times\left[\left[\omega_a^{(D)}-\omega_b^{(D)}-\omega-\sum_j S_j\omega_j\right]^2-\left[\omega_a^{(D)}-\omega_b^{(D)}-2\omega-\sum_j S_j\omega_j\right]^2\right]\right\}\ . \tag{45}$$

Experimentally, χ_e can be determined as follows. For the 0→1 transition we have

$$\omega_{10}=(E_1-E_0)/\hbar=\omega-2\chi_e\omega\ , \tag{46}$$

and for the 1→2 transition we have

$$\omega_{21}=\omega-4\chi_e\omega\ . \tag{47}$$

It follows that

$$\chi_e=(\omega_{10}-\omega_{21})/2\omega\ . \tag{48}$$

It should be noted that in Förster's original treatment the energy-transfer rate constant $W_{a\to b}$ is expressed in terms of the spectral overlap between the emission spectrum of D and absorption spectrum of A. In our problem, it will mean the spectral overlap between the electronic emission spectrum of the F center and the vibrational absorption spectra of the acceptor (i.e., OH^- or OD^- in our case). In treating the F-center–CN^- problem, Fowler[15(b)] also used this spectral overlap expression for $W_{a\to b}$.

C. Calculation of the single-level resonance-Raman scattering cross sections

Now the calculation of the differential scattering cross section will be shown. The quantum states of the system are given by the adiabatic approximation. First start with the usual definition of the differential scattering cross section of the (au)th state[15,16]

$$\frac{d^2\sigma_{au}}{d\Omega\, d\omega_2}=\sum_{av}\frac{d^2\sigma_{au,av}}{d\Omega\, d\omega_2}$$

which is expressed in terms of the cross sections between *au* and *av* states:

$$\frac{d^2\sigma_{au,av}}{d\Omega\, d\omega_2}=\frac{\omega_1\omega_2^3|\mu_1|^2|\mu_2|^2}{\pi\hbar^2c^4}\times\frac{\Gamma_{au,av}|Z_{au,av}|^2}{(\omega_{au,av}-\omega_1+\omega_2)^2+\Gamma^2_{au,av}}\ , \tag{49}$$

where μ_1 and μ_2 are the electronic transition moment matrix elements, $\omega_{au,av}$ is the Raman shift frequency, ω_1 and ω_2 are the incident and scattered light frequency, respectively, and

$$Z_{au,av}=\sum_{v'}\frac{\langle u|v'\rangle\langle v'|v\rangle}{i(\omega_{bv',av}-\omega_1)+\Gamma_{bv',av}}\ , \tag{50}$$

$\langle u|v'\rangle$ and $\langle v'|v\rangle$ are the vibronic overlap integrals.

In Eqs. (49) and (50), u and v represent the vibrational states for the ground electronic states while v' denotes the vibrational states for the intermediate (or resonance) electronic state.

The difficulty in calculating the RRS is in the calculation of $Z_{au,av}$. There are several methods that can be used to calculate $Z_{au,av}$, the one which we used follows closely the derivation of Ref. 17.

In the RRS calculation, we consider two modes; one mode has the average frequency of lattice modes coupled to the F center (those which broaden the F-center absorption), and the second mode is the OH^- or OD^- stretching mode. Because of the strong electron-phonon coupling associated with the average F-center frequency, the calculation is most conveniently done by making a half-range Fourier transform of $Z_{au,av}$, using the short-time approximation, and doing the time integration as in the time-correlator method[18] (rather than taking usual frequency domain approach of explicitly summing over the individual vibrational levels).

V. ANALYSIS OF EXPERIMENTAL RESULTS AND DISCUSSION

To carry out the theoretical analysis of the experimental data, we need to combine Secs. IV A–IV C. By combining the calculations of the population of the various vibronic states of OH^- or OD^- with the calculations of the single-level RRS cross section, the relative intensity of the various vibronic peaks of the RR spectra can be obtained. Then we can compare the intensities of the different vibrational transitions in the theory and relate them to the experimental results for the F-center/OH^- (OD^-) defect pairs.

To calculate the population of the various vibrational excitation, we will use Eq. (8). We can simplify our analysis by assuming that the $(m+1)$th vibrational level decays primarily into mth vibrational level either by radiative or nonradiative vibrational relaxation processes. Thus, Eq. (8) becomes

$$\rho_{mm}=-\left[\frac{\Gamma^{aa}_{mm}}{\Gamma^{mm}_{mm}}\rho_{aa}+\frac{\Gamma^{m+1\,m+1}_{m+1\,m+1}}{\Gamma^{mm}_{mm}}\rho_{m+1,m+1}\right]\ . \tag{51}$$

We have obtained the expression for Γ^{aa}_{mm} in Sec. IV B.

Because of very high OH^- or OD^- concentration in our samples, the decay rate Γ^{mm}_{mm} of the mth vibrational state should consist of two parts; the first part comes from the transition to the lower $(m-1)$ vibrational states; the other comes from the phonon-assisted transition to the neighboring OH^- or OD^- which does not participate in the electronic to vibrational energy transfer. The total decay rate Γ^{mm}_{mm} can be therefore written as[19]

$$\Gamma^{mm}_{mm}=mA+\frac{mB\omega_m^2n(\omega_m)}{\mu_A\mu_D\omega_A\omega_D}\ ,$$

where A, B are constants, ω_m is the anharmonic frequency shift of the mth vibrational level,

$$n(\omega_m)=\frac{1}{\exp(\hbar\omega_m/k_BT)-1}$$

with k_B being the Boltzmann constant, and μ_A,μ_D and ω_A,ω_D are reduced masses and frequencies of the neighboring OH^- or OD^- ions and $F_H(OH^-/OD^-)$ centers, respectively.

We notice that the only fitting parameter from the Γ^{mm}_{mm} term will be the ratio B/A because the experimental results only provide information on the relative intensity of various transitions.

We will now simplify the expression given by Eq. (45). As a reasonable approximation, we can replace ω_j by an average lattice vibrational frequency $\overline{\omega}$ and let $S=\sum_j S_j$ and $\Delta\omega=\omega_a^{(D)}-\omega_b^{(D)}$ to get

$$\frac{W_{a0\rightarrow b2}}{W_{a0\rightarrow b1}}=\frac{\chi_e}{2}\exp\left[\frac{1}{2S\overline{\omega}^2}[(\Delta\omega-\omega-S\overline{\omega})^2-(\Delta\omega-2\omega-S\overline{\omega})^2]\right]\ . \tag{52}$$

Then with Eq. (51) and the realization that the third vibrational state is not populated, i.e., $\rho_{33}=0$ and single level RRS cross sections, we can compute the relative magnitudes of the RRS cross sections of the various transitions for the OH^- or OD^- cases and compare them with the observed experimental results.

The parameter set that gives the best fit to our experimental results is: $\Delta\omega=15\,600$ cm^{-1}, $\overline{\omega}=190$ cm^{-1}, $S=50$, $S'_{OH}=0.01$, $S'_{OD}=0.014$, and $B/A=3.17\times10^{-43}$ g^2. The corresponding fits are shown in Figs. 1 and 2. We notice that these parameters lie within a reasonable range of a pure F center in KCl crystal.

As a further test to our proposed model, we have carried out a comparison between the nonradiative decay rate (as predicted from this theory) and the radiative one. We have found that the former is at least one order of magnitude larger than the latter. These results are consistent with the observed experimental measurements that a sufficient amount of electronic energy has been transferred to OH^- or OD^- so that their vibrational states are populated and detected in our anti-Stokes Raman scattering experiment. Time-resolved RRS experiments on *F*-center–OH^- or –OD^- systems in KCl are currently under way in order to fully test this theory.

Finally, we address the issue of fitting Raman lines *A* and *D*. In principle, these two Raman lines can be fit within our model by assuming that they are the result of light scattering from a widely separated *F*-center–OH^- or *F*-center–OD^- pair defects; however, because of the following reasons, we do not think that this analysis will be informative:

(1) the concentration of this widely separated *F*-center–OH^- or *F*-center–OD^- pair defects, which partially determines the anti-Stokes Raman signal, is not known;

(2) the actual separation distance between the *F* center and OH^- or OD^- is not known in this configuration;

(3) a wide range of the Huang-Rhys coupling constants for the OH^- or OD^- are found to be able to fit the experimental results since the theoretical criterion now is to obtain only the $v=1\rightarrow 0$ transition within the experimental accuracy in each of the defect systems, i.e., *F*-center–OH^- and *F*-center–OD^-.

ACKNOWLEDGMENTS

This work was supported by the National Science Foundation Grants Nos. DMR 87-18228, DMR 87-06416, and CHE-8610104.

---

[1] Y. Yang and F. Lüty, Phys. Rev. Lett. **51**, 419 (1983).

[2] L. Gomez and F. Lüty, Phys. Rev. B **30**, 7194 (1984).

[3] Y. Yang, Wolf von der Osten, and F. Lüty, Phys. Rev. B **32**, 2724 (1985).

[4] P. W. Gash, Phys. Rev. B **34**, 5691 (1986).

[5] P. W. Gash, Phys. Rev. B **35**, 774 (1987).

[6] K. T. Tsen, G. Halama, and F. Lüty, Phys. Rev. B **36**, 9247 (1987).

[7] M. Krantz and F. Lüty, Phys. Rev. B **37**, 8412 (1988). In this paper, a very weak vibrational emission from OH^- has been reported in CsI.

[8] D. J. Jang, M. A. El-Sayed, L. Gomez, and F. Lüty, in *Ultrafast Phenomena V* (Springer-Verlag, Berlin, 1986).

[9] A preliminary report on the experimental results was presented by G. Halama, K. T. Tsen, and F. Lüty at the International Conference on Defects in Insulating Crystals, Parma, Italy, 1988 (unpublished).

[10] B. Wedding and M. V. Klein, Phys. Rev. **177**, 1274 (1969).

[11] Y. Fujimura, Y. Ohtusuki, M. Arai, and S. H. Lin, J. Chem. Phys. **82**, 1246 (1985).

[12] S. H. Lin and H. Eyring, Proc. Natl. Acad. Sci. (USA) **74**, 3623 (1977); B. Fain and S. H. Lin, Surf. Sci. **147**, 497 (1984).

[13] Th. Förster, Ann. Phys. (Lepzig) **2**, 55 (1948); S. H. Lin, Proc. R. Soc. London, Ser. A **352**, 57 (1976).

[14] P. B. Merkel and D. R. Kearn, J. Am. Chem. Soc. **94**, 1029 (1972); A. L. Charles and D. R. Keern, *ibid.* **97**, 2018 (1975).

[15] S. H. Lin, S. T. Lee, Y. H. Yoon, and H. Eyring, Proc. Natl. Acad. Sci. (USA) **73**, 2533 (1976); Y. Y. Lin, Z. T. Chu, and S. H. Lin, J. Photochem. Photobiol. **44A**, 229 (1988). (b) W. B. Fowler (private communication).

[16] Y. Fujimura and S. H. Lin, J. Chem. Phys. **70**, 247 (1979).

[17] Y. Fujimura, S. H. Lin, and H. Eyring, Proc. Natl. Acad. Sci. (USA) **77**, 5032 (1980).

[18] C. K. Chan and J. B. Page, Chem. Phys. Lett. **104**, 609 (1984); C. K. Chan and J. B. Page, J. Chem. Phys. **79**, 5234 (1983).

[19] A. Blumen, S. H. Lin, and J. Manz, J. Chem. Phys. **69**, 881 (1978).